Experimental mechanical strain measurement of tissues

Lingwei Huang[1], Rami K. Korhonen[1], Mikael J. Turunen[1] and Mikko A.J. Finnilä[1,2,3]

[1] Department of Applied Physics, University of Eastern Finland, Kuopio, Finland
[2] Research Unit of Medical Imaging, Physics and Technology, University of Oulu, Oulu, Finland
[3] Medical Research Center Oulu, Oulu University Hospital, Oulu, Finland

ABSTRACT

Strain, an important biomechanical factor, occurs at different scales from molecules and cells to tissues and organs in physiological conditions. Under mechanical strain, the strength of tissues and their micro- and nanocomponents, the structure, proliferation, differentiation and apoptosis of cells and even the cytokines expressed by cells probably shift. Thus, the measurement of mechanical strain (i.e., relative displacement or deformation) is critical to understand functional changes in tissues, and to elucidate basic relationships between mechanical loading and tissue response. In the last decades, a great number of methods have been developed and applied to measure the deformations and mechanical strains in tissues comprising bone, tendon, ligament, muscle and brain as well as blood vessels. In this article, we have reviewed the mechanical strain measurement from six aspects: electro-based, light-based, ultrasound-based, magnetic resonance-based and computed tomography-based techniques, and the texture correlation-based image processing method. The review may help solving the problems of experimental and mechanical strain measurement of tissues under different measurement environments.

INTRODUCTION

Strain is an important mechanical factor that affects strain-associated biological function. Loading of an organ is transferred progressively to smaller scales in a multiscale manner, first to tissues and then to pericellular and cellular levels. At the tissue level, the strains are distributed to the micro- and nanostructure. The structures are optimized to withstand the strains and loads experienced by the tissues. Collagen, a major protein in tissues, contributes to the mechanical properties including ductility under tension but also compressive behavior in many tissues, while mineral crystals provide the rigidity in mineralized tissues, e.g., bone. At the cellular level, mechanical strain can lead to biochemical signal transduction modulating tissue metabolism, and finally influence the function of the organism (*Jacobs, Temiyasathit & Castillo, 2010*). Mechanical strain can then modulate activity and gene expression in cells leading to altered structure and function of tissues.

Mechanical loading exists almost everywhere in cells, tissues, and their matrix components under physiological conditions, which deform under these conditions.

Mechanostat theory, a tissue-level negative feedback system, has two mechanical strain thresholds which determine tissue strength by switching on and off the biological mechanisms (*Frost, 2004*). The strain in tissues induced by mechanical loading can produce fluid flow which influences cells inside the tissues, just as we reviewed before about osteoblasts (*Huang et al., 2015*). Therefore, the judgment of mechanical deformation (i.e., displacement or mechanical strain) is critical to understand functional changes in cells and biological tissues under physiological loading, and to elucidate basic relationships between mechanical strain and the tissue conditions.

At present, texture analysis methods have allowed strain measurement from various imaging methods including optical imaging, magnetic resonance imaging (MRI), X-ray microscopy, and ultrasound (US) imaging, and they are attractive and alternative for traditionally used strain gauge techniques. Recently, reviews on strain characterization include for example *in vivo* strain measurement of bone (*Al Nazer et al., 2012*; *Yang, Bruggemann & Rittweger, 2011*) and ligaments (*Fleming & Beynnon, 2004*) in humans and in-plane strain measurement with digital image correlation (DIC), current methods on strain characterization on bone (*Grassi & Isaksson, 2015*), and the feasibility of non-Doppler US methods with speckle tracking for fetal myocardial strain evaluation (*Germanakis & Gardiner, 2012*). However, these reviews are limited on strain evaluation of one or a few techniques or tissues. Though they can help improving our understanding of the application of some strain assessment techniques in certain tissues, they do not provide a complete review of the state-of-art strain characterization techniques in tissues in general. To provide a relatively comprehensive understanding of various tissue strain measurements and provide a convenient way in choosing a suitable experimental methodology, we reviewed the mechanical strain measurement techniques from six aspects: electro-based, light-based, ultrasound-based (US-based), magnetic resonance-based (MR-based) and computed tomography-based (CT-based) techniques, and the texture correlation-based (TC-based) image processing method. The review may help interpreting and debugging problems and challenges of mechanical strain estimation in biological tissues during experiments and clinical applications. Furthermore, this review might aid in choosing adequate mechanical strain estimation tools for a study based on the listed pros and cons.

SURVEY METHODOLOGY

To search the available reports on the experimental and mechanical strain measurement of biological tissues, a standardized search strategy was conducted to survey studies indexed in PubMed and Web of Science databases. The search terms were selected as "strain", "deformation", and "tissue", together with "measurement", "evaluation", and "quantification". We strictly searched for publications focusing on the experimental and mechanical strain measurement of tissues that represent the state-of-art methodology and that are continuously used in current research. Research published before November 2018 were collected based on our criteria. After excluding the strain measurement of artificial materials and the strain measurement in cell, molecule or atom level, and removing the old fashioned or modeling of strain, 143 articles were selected in our manuscript, among which,

there were 10 physiological mechanical strain related introduction articles, 37 electro-based mechanical strain measurement articles, 12 light-based mechanical strain measurement articles, 21 US-based mechanical strain measurement articles, 16 MR-based mechanical strain measurement articles, 12 CT-based mechanical strain measurement articles, 42 TC-based image processing articles. In seven articles, different strain measurement techniques were compared or combined.

SUMMARY OF THE MECHANICAL STRAIN MEASUREMENT

Six types of tissue strain assessment approaches including electro-based, light-based, US-based, MR-based and CT-based techniques, together with the TC-based image processing method were analyzed. The mechanisms and possibilities of different techniques for the strain measurement in various tissues have been summarized in Table 1 and further explained in the following chapters.

ELECTRO-BASED MECHANICAL STRAIN MEASUREMENT

Electro-based mechanical strain measurement techniques are widely used for the evaluation of tissue deformations. Especially, the strain gauge technique is commonly applied as a golden standard in the mechanical strain measurement of tissues. In the following parts, all the electro-based mechanical strain measurement techniques are treated as ''strain sensors''.

The principle of electro-based mechanical strain measurement

This technique is built on the electrical resistance change of the strain sensors. When a tissue deforms, the electrical resistance of strain sensors inserted or attached to the tissue will change, which results in changed output electrical signal. The electrical signal, which is proportional to the tissue deformation, is amplified and detected with a signal acquisition device (e.g., MP160WSW, BIOPAC, USA) and then the signal is collected with a related software in a computer as digital data. Finally, the collected data is converted into mechanical strain value. There are various types of strain gauges including bare strain gauges (without coating layers), coated strain gauges, strain transducers, instrumented strain gauges, and differential reluctance transducers. Bare strain gauges are extensively applied for *ex vivo* or temporarily *in vivo* mechanical strain measurement of hard tissues including bone (Fig. 1). Coated strain gauges consisting of hydroxyapatite-coated (HA-coated), calcium phosphate ceramic-coated (CPC-coated) and resin coated strain gauges, are verified and available for *in vivo* mechanical strain measurement of tissues, especially bone. Strain transducers are usually composed of polymers and are universally used for the mechanical strain measurement of soft tissues such as ligament, nerve and cartilage. Differential reluctance transducers are created on the varying magnetic flux with their deformation caused by tissues and the altered magnetic flux will be transformed into electrical signals for mechanical strain assessment of surrounding tissues. Instrumented screws can be used to record mechanical strain and they are widely applied for the mechanical strain evaluation of hard tissues, especially those with irregular shapes.

Table 1 Mechanisms of strain measurement for different methods and their possible applications

Type	Approach	Mechanism of mechanical strain evaluation	Strain range	Test	Target tissue	Reference examples
Electro-based	Strain gauge Strain transducers	The deformation of tissues induces the electrical signal changes, which can be converted into strain values of the tissues.	$10\sim10^7\mu\varepsilon$	Discrete *In vivo* *Ex vivo*	Bone Cartilage Ligament Tendon Muscle	*Takano et al. (1999)* *Szivek, Anderson & DeYoung (1997)* *Pintar et al. (1995)* *Rolf et al. (1997)* *Markolf et al. (1998)*
Light-based	Microscopy camera	The relative strain is assessed by comparing the images before and after the tissue deformation.	$10^2\sim10^6\mu\varepsilon$	Serial *Ex vivo*	Cartilage Ligament Tendon Nerve Blood vessel	*Moo et al. (2018)* *Wright et al. (1996)* *Bartell et al. (2015)* *Teo, Dutton & Han (2010)* *Butler et al. (1990)* *Squire, Rogers & Edelman (1999)*
US-based	Tissue Doppler imaging	The strain is calculated from US images of the tissues, according to the Doppler effect (frequency shift) of the reflected US incited by the deformation of tissues.		Serial *Ex vivo* *In vivo*	Myocardial wall Gastric wall Vascular wall	
	US elastography	The strain of tissues is assessed by the correlation of the pulsed US echo signals in windows before and after tissue deformation.	$10^3\sim10^6\mu\varepsilon$	Serial *In vivo* *Ex vivo*	Myocardial wall Gastric wall Vascular wall Cartilage Tendon Ligament	*Perk, Tunick & Kronzon (2007)* *O'Neill et al. (2007)* *Ling, Zheng & Patil (2007)* *Amundsen et al. (2006)* *Gilja et al. (2002)* *Liang, Zhu & Friedman (2008)* *Wilson, Press & Zhang (2009b)* *Bihari et al. (2013)*
	Speckle tracking echocardiography	Strain is quantified from changed reflection US interference patterns in the US images during the deformation of the tissues.		Serial *In vivo* *Ex vivo*		

Table 1 (*continued*)

| Type	Approach	Mechanism of mechanical strain evaluation	Strain range	Test	Target tissue	Reference examples
Magnet-based	Tag tracking MRI	The applied magnetization tags in the tissues change with the deformation of tissues and strain messages can be extracted from the changed images of tags.	$10^2 \sim 10^6 \mu\varepsilon$	Serial *In vivo* *Ex vivo*	Myocardium Bone Cartilage Tendon Ligament Liver Brain	*Axel (1997)* *Al Nazer et al. (2008)* *Sutter et al. (2015)* *Sheehan & Drace (2000)* *Mannelli et al. (2012)* *Hirsch et al. (2013)*
	Elastography MRI	Strain is assessed from changed signal patterns in MR images obtained from the tissues before and after their deformation.		Serial *In vivo* *Ex vivo*		
CT-based	CT	Strain values are acquired from the changes of reconstructed 3D structure of tissues before and after deformation.	$10 \sim 10^4 \mu\varepsilon$	Serial *In vivo* *Ex vivo*	Bone Cartilage Heart Calcified cartilage Blood vessel	*Novitskaya et al. (2014)* *Halonen et al. (2014)* *Pierce et al. (2016)* *Boekhoven et al. (2014)* *Gustafsson et al. (2018)*
TC for image processing	DIC	Strain is evaluated by tracking the subsets including markers or speckles on the surface of tissues.	$10^2 \sim 10^4 \mu\varepsilon$	Serial *Ex vivo*	Bone Blood vessels Other tissues with marked surface	*Hussein, Barbone & Morgan (2012)* *Sheehan & Drace (2000)* *Bey et al. (2002a)* *Cyganik et al. (2014)*
	DVC	Strain is evaluated by tracking image subsets by tracking the natural pattern in the tissues.		Serial *In vivo* *Ex vivo*	All tissues with specific structure features	*Bay (1995)* *McKinley, English & Bay (2003)* *Bay et al. (1999)* *Toh et al. (2006)*
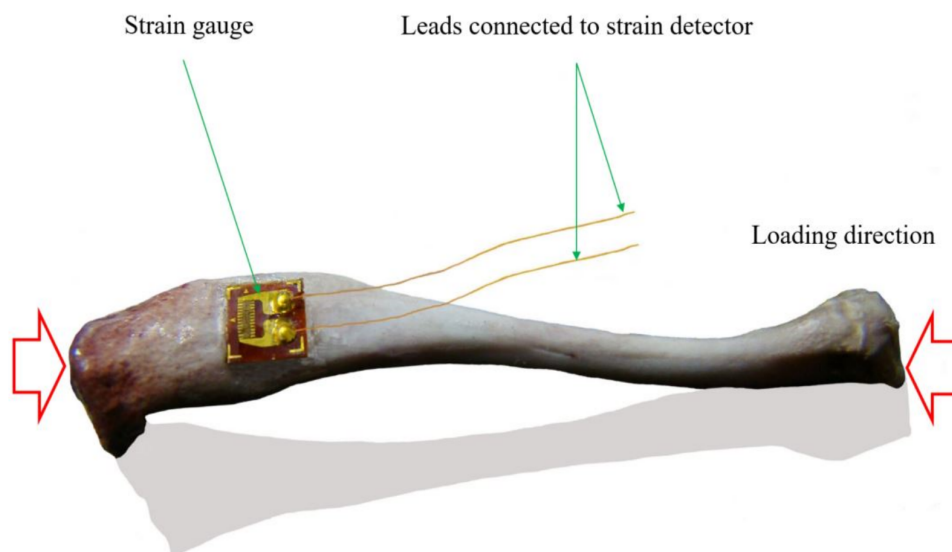
Figure 1 Schematic view of the axial strain measurement of tibia with single strain gauge. When bone deforms, the attached strain gauge will deform, and the embedded metal strain resistance wire will deform too, resulting in the resistance change of the metal strain resistance wire and finally resulting in changed output signals, and the changed signals can be transferred into strain using a strain detector (this figure was generated from a rat tibia by a Lingwei Huang).

Full-size 🖼 DOI: 10.7717/peerj.6545/fig-1

The application of electro-based mechanical strain measurement
Strain gauge

Ex vivo mechanical strains around natural teeth with prostheses and at femoral necks and metatarsals in human cadavers were evaluated with strain gauges bonded on bone during mechanical loading (*Cehreli et al., 2005*; *Enns-Bray et al., 2016*; *Fung, Loundagin & Edwards, 2017*). In one *ex vivo* experiment, four triple strain gauge rosettes were used to measure the mechanical strain of metacarpus and distal row of horse carpal bones (*Les et al., 1998*). Rosette strain gauges were also used to study the mechanical strain shielding of plates in sheep tibias with rosette strain gauges fixed onto the anterior and posterior aspects of the tibias (*Gautier, Perren & Cordey, 2000*). In another study, three strain gauges were placed around the mid-shaft of the radius of foxhounds to find the relationship of peak functional and mechanical strains of bone (*Takano et al., 1999*). Because of electrical signal disturbance caused by intracorporal environment, common strain gauge applications without the protection of coat layers are limited. Dielectric material coated strain gauges and instrumented strain gauges are developed to reduce the influence of *in vivo* environment on the transduction of electrical signals in strain gauges and are widely utilized for *in vivo* mechanical strain measurement.

Coated strain gauges
The bonding of HA-coated strain gauges and bone was analyzed with cantilever bending test by comparing the strain change after 6–7 weeks' adhesion, and 70–100% bonding was found between HA-coated strain gauges and rat femur (*Wilson et al., 2009a*). Another study

in greyhound femur showed well-bonded and sensing accuracy after 4-month implant of the coated strain gauges (*Szivek et al., 1990*). CPC-coated strain gauges were also exploited to accurately measure bone mechanical strain *in vivo* during exercises (*Rabkin et al., 2001*). *In vivo* and *ex vivo* mechanical strain evaluation of the proximal femora of dogs at a series of gait speeds using CPC-coated strain gauges showed that mechanical strain patterns were similar and peak mechanical strains were the same in the following 2 weeks (*Szivek, Anderson & DeYoung, 1997*). Resin coated rosette strain gauges could also be exploited to measure surface mechanical strain on the dorsomedial cortex of the third metacarpal bones in six adult horses during treadmill exercise (*Davies, Mccarthy & Jeffcott, 1993*).

Strain transducers

In one study, the strain transducers were implanted into medial and lateral ligaments of the ankles harvested from human cadavers to measure mechanical strain changes of the ankle ligaments (*Ozeki et al., 2002*). In another study, the mechanical strain in the anteromedial band of the anterior cruciate ligament of thirteen fresh frozen cadaveric knee specimens was also measured using transducers with barbed prongs inserted into the anteromedial band to record local elongation of the instrumented fibers (*Markolf et al., 1998*). Further, Pozzi *et al.* inserted subminiature differential variable reluctance transducers into the periphery of the caudal pole of the menisci of adult dogs to measure the mechanical strain of the caudal region before and after loading under meniscectomies (*Pozzi, Tonks & Ling, 2010*). Also in one human cadaver study, differential reluctance transducers have been placed in the superficial peroneal nerve in sixteen lower-extremity specimens to measure mechanical strain *in situ* to find the strain variation in the intact and the sectioned anterior talofibular ligaments during a simulated inversion sprain (*O'Neill et al., 2007*). In another human study, the mechanical strains of the anterior cruciate ligaments were measured using a differential variable reluctance transducer attached, during closed kinetic chain exercises (*Heijne et al., 2004*) and simulated movement (*Hacker et al., 2018*).

Instrumented strain gauges

In human studies, surgical staples with two strain gauges were inserted through skin incision into the cortical bone of tibia to measure local bone deformation *in vivo* under static conditions (*Rolf et al., 1997*), and during exercises (*Milgrom et al., 2000a*; *Milgrom et al., 2000b*). In clinical practice, strain gauges were attached to the fixation rod of 500 bone fracture patients with external bone fixator to measure the rod deformation when raising the limb to a given angle in the healing process (*Burny et al., 1984*), so that the bone deformation beneath the fixator could be evaluated. Linear relationship was found between the calculated mechanical strain at the bone surface and the strain measured by the instrumented bone staples, suggesting instrumented staples' effectiveness for local bone deformation measurement (*Ekenman et al., 1998*). Even so, higher mechanical strain was observed at the bone-screw interface in the end regions of an anterior solid rod construct during lateral bending (*Spiegel et al., 2000*).

Electro-based techniques are widely used as principle methods for mechanical strain measurement. Nevertheless, the techniques are limited to superficial or simple mechanical strain measurement of tissues. Also, the precision of the measurement is largely dependent

on the quality of the strain sensors themselves and their attachment, and the attached strain sensors can also affect the deformation of a sample to some degree.

LIGHT-BASED MECHANICAL STRAIN MEASUREMENT

Light-based mechanical strain measurement is a non-contacting strain evaluation method.

The principle of light-based mechanical strain measurement

Light-based mechanical strain measurement is established on extracting tissue strains from deformation induced change of optical information (e.g., image datasets). During the deformation, the markers and special features in tissues are tracked and recorded with laser beam and image recorders respectively. Then, the markers' movement or the features' change is evaluated between those before and after deformation. Finally, mechanical strains are extracted from the changed markers' positions or features' characteristics according to image processing algorithms.

The application of light-based mechanical strain measurement

High speed camera and confocal laser scanning microscopy can be used to measure localized deformation of cartilage or other tissues via comparing the alterations of gathered pictures. Bulk mechanical strain was recently calculated using the image taken at peak indentation and the image before deformation (*Bartell et al., 2015*). Confocal laser scanning microscopy combined with image analysis could also measure global, local axial and transverse mechanical strains of cartilages *in situ* (*Fick et al., 2016*; *Fick et al., 2015*; *Turunen et al., 2013*), by tracking markers in the tissues, i.e., cells (*Mansfield, Bell & Winlove, 2015*). Analogously, the surface deformation of human ulnar collateral ligament was studied by tracking the artificial markers fixed on the tissue surface during mechanical testing (*Smith et al., 2019*). Recently, a novel method was used to quantify three dimensional (3D) tissue strain of intact cartilage in *ex vivo* pig knees at sub-micrometer resolution (*Moo et al., 2018*). In this microscopic technique, a 3D grid is imprinted into fibrous tissue and strain can be quantified by imaging the grid deformation at various strain/stress levels.

US-BASED MECHANICAL STRAIN MEASUREMENT

Ultrasound is popularly adopted for non-destructive mechanical strain estimations of tissues both *in vivo* and *ex vivo*. US-based mechanical strain measurement can be mainly divided into tissue Doppler imaging (tissue Doppler echocardiography), US elastography and speckle tracking echocardiography. US imaging or sonography is often exploited in the mechanical strain assessment of tissues.

The principle of US-based mechanical strain measurement

In ultrasonic imaging, US is emitted into tissues and the echoed US is recorded and displayed as images. By comparing the recorded images before and after the deformation of the tissues, strain information can be extracted. Familiarly, pulsed US is employed in US imaging due to its high signal-to-noise ratio. There are various US elastography techniques that also allow strain quantification. One benefit of US is that besides imaging deformation caused by

external loading, also deformation caused by physiological processes or US radiation can be utilized for elastography. The mechanical strain of tissues is assessed by the correlation of the pulsed US echo signals in windows before and after tissue deformation. For speckle tracking echocardiography, the reflected US produces constructive and destructive interferences, and the interferences (i.e., speckles) will redistribute during the deformation of the tissues, which leads to relative displacements of the interference patterns in the US images, and the displacements are tracked for the assessment of tissue deformations. For tissue Doppler imaging, US with a high frequency creates an image of the tissues, according to the Doppler effect (frequency shift) of the reflected US incited by the deformation of tissues.

The application of US-based mechanical strain measurement

US can be used in mechanical strain measurement by Doppler-based or Non-Doppler-based techniques. The Doppler-based technique is angle dependent, whose measurement can be only done along the orientation of ultrasonic beam. While Non-Doppler strain imaging is angle independent and can be used for clinical mechanical strain measurement of myocardial wall (*Perk, Tunick & Kronzon, 2007*).

In vitro research on bovine articular cartilage showed that US speed in the sample was highly correlated to the applied mechanical strain in a quadratic relation and ultrasound speed changed by 7.8% when the applied compression strain reached 20% (*Ling, Zheng & Patil, 2007*), which showed close relationship between strain value and the change in US speed. Speckle tracking echocardiography was validated as a method for *in vivo* angle-independent measurement of regional myocardial strain of humans (*Amundsen et al., 2006*). Strain rate imaging, a method in echocardiography, was employed for radial deformation measurement of human left ventricle (*Herbots et al., 2004*). Similarly, two dimensional (2D) myocardial deformation of human left ventricles was estimated using the angle-independent myocardial elastography (a radio-frequency based speckle tracking technique) and the tagged MRI, and the deformation estimations by the two methods were in good agreement with each other (*Lee et al., 2008*). Multidimensional radio-frequency echo phase matching method was also applied to measure deformations in the lateral and axial directions (*Sumi, 2007*). In addition, transabdominal strain rate imaging, a Doppler US method was utilized to explore the mechanical strain of the muscle layers within the gastric wall during gastric contractions in humans (*Gilja et al., 2002*).

Additionally, radiofrequency US-based imaging techniques were devoted for radial and longitudinal mechanical strain measurement of the sub-endocardial, mid-wall and sub-epicardial layers of tissues from healthy and infarcted regions in five pigs (*Van Slochteren et al., 2014*). Intravascular US elastography was enhanced by developing a 2D mechanical strain estimation method to acquire the strain tensor that reflects mechanical strains in any direction in the cross-section of artery wall (*Liang, Zhu & Friedman, 2008*). Ultrasonography imaging in combination with computational methods was applied for the mechanical strain measurement of human Achilles tendons (*Peltonen et al., 2013*; *Stokes et al., 2010*) and quadriceps tendons (*Wilson, Press & Zhang, 2009b*) *in vivo*, and rabbit Achilles tendons *ex vivo* (*Kuo et al., 1999*). The procedure varies among different US systems for mechanical strain measurement. Investigation of two echocardiograms of

patients from two different commercial US systems showed that post-processing is the most important determinant in inter-vendor variation (*Negishi et al., 2013*).

Universally, US-based mechanical strain measurement is a promising method for simple strain assessment of tissues, especially clinically. 3D strain inside the tissues, especially for heterogeneous or irregular tissues, cannot be evaluated, though 3D echocardiography has been devoted for 3D cardiac deformation estimation, utilizing an algorithm concerning a transversely isotropic linear elastic model (*Papademetris et al., 2001*). A real-time 3D speckle tracking US was established to explore the local wall strain of the whole abdominal aortic aneurysm in patients *in vivo* (*Bihari et al., 2013*). US tomography approach (echo-computed tomography) could be also applied to estimate local deformations of human carotid using a 2D mechanical strain algorithm, and 3D radial mechanical strain data was reconstructed (*Boekhoven et al., 2014*).

MR-BASED MECHANICAL STRAIN MEASUREMENT

Magnetic resonance based mechanical strain measurement techniques mostly focus on the mechanical strain measurement with MRI, though another system presented its capability in monitoring the real-time deformation of intracranial brain during impact-induced brain injury of rats through detecting the changing magnetic field produced by the movement of implantable soft magnet (*Song et al., 2015*). MRI can be divided into MR elastography and MR tag tracking in accordance with the integrated techniques. Because of no negative effects reported, MRI is looked as a reliable and secure way for the mechanical strain evaluation of brain, heart, and other important tissues where the tissue strains are difficult to be investigated with other mechanical strain measurement techniques without side effect on the organisms *in vivo*.

The principle of MR-based mechanical strain measurement

There are specific sequences (e.g., DENSE) for mechanical strain imaging. Alternatively, deformation of tissues can be assessed by following the magnetization tags in the tissues or evaluating the changes of signal patterns with texture correlation (TC) image processing methods.

The application of MR-based mechanical strain measurement

MRI is based on magnetization tags (temporary features in tissues produced by a special pulse sequence and moving with the tissues) tracing and mechanical strain-induced phase shifts in tissues (*Axel, 1997*) which can be translated into the deformation of the tissues. MRI with tagging is generally used for noninvasive myocardial strain assessment with acceptable accuracy (*Lima et al., 1993*). The assessment of cardiac deformation by cardiovascular MRI combined with feature tracking has been validated feasible in children (*Andre et al., 2016*). Cardiac MRI was developed for measuring peak systolic circumferential strain (*Simonetti & Raman, 2010*) and intramyocardial strain (*Axel, 1997*). In addition, a transmural gradient in the mechanical strain of a normal dog heart was detected with MRI together with multispectral radio-frequency pulses produced tagging grids for high-resolution mechanical strain estimation (*McVeigh & Zerhouni, 1991*). With magnetization tags, MRI was also used

to quantify the cardiac induced liver strain and the head's angular acceleration produced brain strain in humans (*Chan et al., 2018*; *Mannelli et al., 2012*). Motion-sensitive phase contrast MRI was applied for the measurement of volumetric strain of brain (*Hirsch et al., 2013*) and patellar tendons (*Sheehan & Drace, 2000*) in humans as well. Using MRI and image registration techniques, *in vivo* 3D deformation of cervical spinal cord in rat was quantified (*Bhatnagar et al., 2016*). MRI could also be used to measure local tibiofemoral cartilage strains in response to a dynamic hopping activity (*Sutter et al., 2015*) and the dynamic mechanical strains in tibia during human locomotion (*Al Nazer et al., 2008*), combined with an iterative closest point technique (i.e., MR tag tracking) and a flexible multibody approach (i.e., MR elastography) respectively. Besides, MR-based technique was utilized to quantify intratendinous mechanical strains in cadaveric shoulder specimens at superior, middle, and inferior locations across the regions where most rotator cuff tears occur clinically (*Bey et al., 2002a*).

CT-BASED MECHANICAL STRAIN MEASUREMENT

Computed tomography (CT) is a very common technique in 3D structure characterization of tissues. The main parts of the CT are X-ray sources, detectors and associated software for reconstruction and visualization, and possibly for structural and mechanical strain analysis.

The principle of CT in mechanical strain measurement

First, projection images of the tissues before and after deformation are acquired. This can be a time consuming process especially with a high-resolution experimental system. Then, the original images are reconstructed and modeled into 3D structures of the tissues (one of the tissues before deformation and one of the tissues after deformation). Finally, the strain information of the tissues can be evaluated through comparing the tissues' structure before and after deformation.

The application of CT in mechanical strain measurement

With contrast media, a novel cone beam CT-scanners combined with an analyzing software was applied to study the mechanical strain of articular cartilage in human knees during static loading (*Halonen et al., 2014*). Similarly, micro-computed tomography (micro-CT) scanner could be applied to evaluate mechanical strain in human cadaveric meniscal tissues by tracking small Teflon markers implanted (*Kolaczek et al., 2016*) and assess large deformations of ovine hearts by tracking fiducial markers applied (*Pierce et al., 2016*). The creep deformation of human trabecular bone samples from proximal tibia was assessed as well by analyzing the tissue architecture both before and after creep using micro-CT imaging (*Novitskaya et al., 2014*).

TC-BASED IMAGE ANALYSIS OF MECHANICAL STRAIN

Texture correlation is a widely utilized image processing method for the characterization of changes in structure, i.e., tissue deformation. This strain evaluation method in tissues depends on the comparison of images from the tissues before and after deformation.

DIC

DIC is a TC-based method for non-contact, superficial deformation measurement (*Kahnjetter & Chu, 1990*) and can be used basically with any imaging modality. This method is increasingly used for *in vitro* set-ups (*Shelton & Katz, 1991*), and is particularly suitable for biological applications in view of its accurate mechanical strain measurement in inhomogeneous, anisotropic, non-linear materials, such as mandible (*Tanasic et al., 2012*).

The principle of DIC

DIC is an appropriate image processing method for assessing mechanical strain distribution throughout the structures with complex geometries (*Rodriguez et al., 2004*). The basic principle of DIC is to co-register the same physical points between the two images recorded before and after deformation (Fig. 2). A square reference subset centered at the interrogated point in the reference image is chosen and used to track its corresponding location motion. The displacement field can be determined by the calculations with a derivative algorithm. To evaluate the similarity degree between the reference and target subsets, a certain correlation criterion should be defined in advance (*Dai et al., 2015*). In general, zero-mean cross correlation criterion (*Pan et al., 2009*) is used. In some other similar methods, high contrast markers are sprayed onto the surface of the sample and observed with cameras during loading. The entire field of view is divided into a number of unique correlation areas, or 'facets', which typically contain a square subset of pixels. The characteristic features of the speckle pattern in the facets will be tracked during loading and the modified features provide a progressive measurement of deformation (*Tanasic et al., 2012*).

The application of DIC in mechanical strain measurement

2D image processing DIC combined with a high-quality imaging device is widely used for in-plane mechanical strain measurement as an effective and irreplaceable method (*Pan et al., 2009*). Combined with DIC, an experimental microextensometry approach has been developed to analyze the displacement and mechanical strain fields on the surface of the mature bovine cortical bone (*Hoc et al., 2006*). Besides, a series of images from ring porcine aorta surface were analyzed to quantify the local surface strain of vascular tissues subjected to ramped uniaxial loading (*Bey et al., 2002a*). Similarly, the displacement and full-field mechanical strain in human femoral heads and mouse forearms have been evaluated *ex vivo* using DIC, combined with camera images before and after mechanical loading (*Begonia et al., 2015*; *Cyganik et al., 2014*). The mechanical strain evaluation method of DIC is confined to 2D and some speckles under tracing may be missing, introducing challenges of evaluating the strain of tissues with curved surface.

To overcome the limitations of plain mechanical strain measurement of DIC, practical and effective 3D image processing approach DIC or digital volume correlation (DVC) has been developed for the strain measurement of tissues with both planar and curved surface (*Pan et al., 2009*). The uncertainties of DVC have been demonstrated acceptable combined with images from X-ray micro-CT and optical scanning tomography (*Germaneau, Doumalin & Dupré, 2008*).
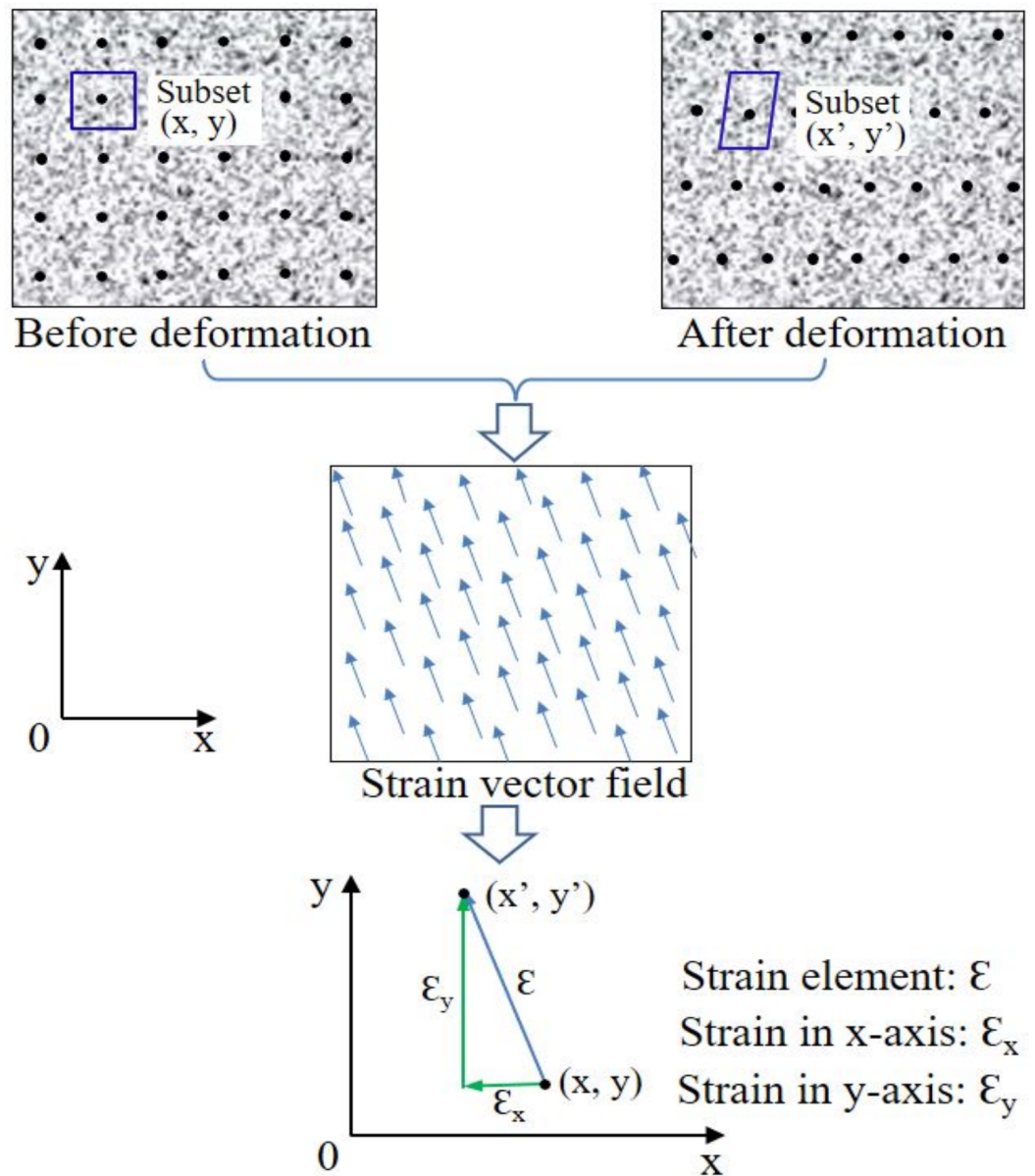
Figure 2 Principle of 2D strain measurement of region of interest in samples using DIC. Comparing the target and reference regions (consisting of subsets with speckles (black points in sample images) inside) of the sample, the varied characteristic features can be acquired and then converted into strain. Adapted from *Dai et al. (2015)*.

Full-size ◰ DOI: 10.7717/peerj.6545/fig-2

DVC

DVC is an extension of DIC and its applications have been reviewed previously (*Bay, 2008*). DVC is an image processing method that quantifies mechanical strains throughout the interior of the tissues, rather than simply on the surface, contributing to 3D mechanical strain evaluations. This technique relies on tracking the movement of structural features of tissues with subsets of voxels, rather than with subsets of pixels.

The principle of DVC

Similar to DIC, in DVC, voxels of the natural texture in biological tissues are utilized for the evaluation of mechanical strain fields between two consecutive digital images. This technique was developed and validated with six samples of trabecular bone from a single human femoral head, in which the motion of subsets within images was tracked and the displacement was acquired by comparing images of the initial (i.e., reference) and current (i.e., deformed) configuration (*Bay, 1995*).

The application of DVC in mechanical strain measurement

Mechanical strains of trabecular bone in the proximal and distal tibia and central vertebrae of human cadavers under mechanical loading were studied with DVC of radiographs from the bone with unloaded and different loaded conditions (*Bay et al., 1999*; *McKinley & Bay, 2001*; *Gillard et al., 2014*). DVC, together with contact radiographs of the tissues, was applied for mechanical strain measurement of specimens from proximal medial tibia of human cadavers under loading, and sharp rises in trabecular bone strain were found under increased subchondral bone defects (*Brown, McKinley & Bay, 2002*), complete meniscectomy (*McKinley, English & Bay, 2003*), or simulated subchondral stiffening (*McKinley & Bay, 2003*). Similarly, local mechanical strain fields in the mid-diaphyseal cortical bone of canine femurs (*Kim, Brunski & Nicolella, 2005*) and local distribution of minimum principal strain and maximum shear strain of intact (*Yerby et al., 1998*) and pedicle screw implanted thoracic spines of human cadavers (*Toh et al., 2006*) under mechanical loading were investigated with machine vision photogrammetry and digitized contact radiographs respectively, with DVC technique.

Presently, many micro-CT combined DVC have been presented for the mechanical strain quantification of tissues. DVC has been verified for 3D measurement of the deformation in *ex vivo* porcine lamina cribrosa, retrolaminar neural tissue and vertebrae under different mechanical loading conditions using images acquired from micro-CT (*Coudrillier et al., 2016*; *Danesi, Tozzi & Cristofolini, 2016*; *Feola et al., 2017*). In addition, the deformation in the spine of human and rats under mechanical loading was measured using deformable image registration algorithm combined with micro-CT (*Choudhari et al., 2016*; *Hussein, Barbone & Morgan, 2012*).

DISCUSSIONS AND CONCLUSIONS

At present, various techniques consisting of optical imaging, MRI, X-ray scanning imaging, US imaging, and strain gauge technique, together with the TC-based image processing method, are familiarly taken for mechanical strain measurement of tissues comprising bone, tendons, ligaments, muscles, brain tissues and blood vessels. The characters and some applications of these techniques have been evaluated in Table 2.

The strain gauge method, one of the electro-based mechanical strain measurement techniques, is usually considered as a gold standard in bone strain measurement. The size of a typical strain gauge is several millimeters, staying in macroscopic level. In some conditions, the tissue surface is not big enough for the attachment of strain gauge. Miniature strain gauges can reduce the attaching area needed and have been employed for the mechanical

Table 2 Information of the main methods for the mechanical strain measurement of tissues.

Technique	Dimension	Advantage	Disadvantage	Operation time	Image analysis
Strain gauge	2D	Cheap;	Invasive;	Real-time	N/A
Strain transducers	3D	Few offline work	Low anti-interference		
Microscopy	2D	Cheap;	Transparent or	Range from minutes	Marker-tracking
camera	3D	Easy operation	translucent samples	to hours	algorithm
Tissue Doppler imaging	1D				
	2D				
US elastography	2D	Cheap; Easy clinical application	Simple structure	Minutes	Baseband speckle-tracking algorithm; Registration algorithm
Speckle tracking echocardiography					
Tag tracking MRI	3D	Safe and no side effect	Expensive;	Range from minutes	Registration algorithm
Elastography MRI			Time-consuming	to hours	
CT	3D	Relatively fast imaging; Relatively low cost	High contrast tissues needed; X-ray radiation	Range from seconds to hours	Registration algorithm

Notes.
[a] Most of the image analysis methods are TC-based; please see example references from Table 1.

strain measurement of a human cadaver cervical vertebral (*Pintar et al., 1995*) or condylar neck of miniature pigs during normal or simulated function (*Marks et al., 1997*). In clinical studies, miniature three-element rosette strain gauges were mounted on the medial and lateral surfaces of human patella and significant mechanical strain redistribution was found after graft removal (*Steen et al., 1999*). When the thickness of the epoxy film of the strain sensors cannot be ignored, it may influence the validity of measurement results of the mechanical strain. The mechanical behavior of thin film was measured and was found that the influence of the thin film can be ignored (*Wang et al., 2014*).

To minimize the influence of strain sensors on tissues' mechanical strain survey, film sensors may be another good choice, though most of these techniques are applied in material engineering. Just like pure transducers (*Bravo, Tersalvi & Tosi, 1992*), the deposition of the strain gauge directly on the mechanical support by using the thin-film technique, instead of gluing on it a strain gauge laminated on polymeric foil, may provide a great improvement in sensor performance. A highly-sensitive and ultra-thin silicon stress sensor whose sensitivity is around 70 times that of metal strain gauge, are demonstrated flexible and sensitive enough for the measurement of mechanical strain on curved surfaces of human bodies (*Zhao et al., 2014*). Additionally, a novel flexible implantable device with higher sensitivities than those of commercial gauges has been applied for real-time mechanical strain measurement of chicken tibiae under three-point bending. Semiconductor strain sensors which are fabricated on flexible polyimide substrates, have significantly reduced sensor size and power consumption compared to metallic foil strain sensors and further decreased their effect on tissues' deformation (*Lisong et al., 2006*).

To acquire immediate mechanical strain information of tissues *in vivo*, implantable and coated strain gauges with subminiature radio transmitter have been created. The

telemetry measurement has been already verified available with the *in vivo* mechanical strain quantification of human cadaver spines during anteroposterior bending and torsion, though a small time shift occurred (*Szivek et al., 2002*). Whereas, all the elecro-based mechanical strain measurement techniques demand the insertion or attachment of sensors to target tissues and the soft tissues make it hard to manipulate. The application of wearable devices for the detection of real-time mechanical strain is becoming a potential method of health care.

The electro-based mechanical strain measurement, as an invasive method, determines the strain of tissues discretely and the strain it obtains is the average value of the measured regions. An investigation of the averaging effect showed limitations in adequate compensation and avoiding of the error magnitudes (*Younis & Kang, 2011*). Moreover, large deformation may produce damage of the circuit elements on rigid islands connected by stretchable wires, and the presence of rigid areas within the substrate limits its deformation. Though a wireless strain gauge was recently developed for remote mechanical strain measurement to eliminate the effect of wires, the range of measurable values decreased as the distance between the sensor and the reading unit increased (*DiGiampaolo, DiCarlofelice & Gregori, 2017*). Super thin substrate may provide a good solution (*Sekitani et al., 2010*). For curve mechanical strain measurement, fiber Bragg grating sensors were presented for the measurement of the bending curvatures of polyimide thin film skin with 48 sensors glued on the skin surface (*Sun et al., 2018*). Though mechanical strains at other regions can be calculated in conjunction with the cross-sectional area of the specimens, the computed values are probably different from those of actual strain distributions owing to the complex and heterogeneous structure in the samples. The accuracy of electro-based mechanical strain measurement techniques highly depends on the quality of strain sensors and their attachment or insertion to the tissues.

US-based methods are widely applied clinically as noninvasive techniques for mechanical strain measurement *in vivo*. Strong correlations were found between DIC and US radiofrequency elastographic estimates of mechanical strain (*Chernak Slane & Thelen, 2014*). Tissue Doppler imaging is highly angle-dependent and is for the mechanical strain testing of tissues in the direction parallel to US beam, while speckle-tracking echocardiography can track the tissue strain not restricted to the direction parallel to the US beam. In 2D speckle-tracking echocardiography, the tracked speckles may be missing in the tracking plane, which can be solved by 3D speckle-tracking echocardiography. The comparison of 2D speckle-tracking echocardiography and 3D speckle-tracking echocardiography has been reviewed already (*Muraru et al., 2018*), and the longitudinal and apical foetal speckle tracking echocardiography of the foetal heart in gestational woman was conducted for strain assessment with tissue motion annular displacement and segmental longitudinal strain (*Derpa et al., 2018*). Because US-based mechanical strain measurement techniques are built on US reflection, the mechanical strain of the tissues with complex and un-uniform structure can't be evaluated precisely using the US-based mechanical strain measurement techniques.

MR-based methods can be utilized to test dynamic strain with a resolution of around 0.1 mm. For MRI, motion-induced phase shifts technique is with greater precision than

the tag displacement measurement (*Axel, 1997*). No side effects have been found during the mechanical strain measurement with MRI, which indicates the latent ability for clinical use. However, due to the resolution of MRI, this technique has limitations in a small-scale local strain analysis. MR-based mechanical strain measurement is also expensive and time-consuming, which decreases its value as a clinical application.

The light-based mechanical strain measurement can only be used for superficial mechanical strain measurement or the mechanical strain measurement of transparent or translucent tissues due to the disability of optics to penetrate tissues. Their easy-operation, time-saving and low-cost prompt their applications in clinical practice and laboratories. A multi-camera speckle interferometer was lately developed and optimized for the full-field displacement measurement of human eye sclera during inflation testing (*Bruno, Bianco & Fazio, 2018*), suggesting the application of light interference.

In DIC, the imaging configurations play a vital role in the preciseness of mechanical strain measurement (*Zhu et al., 2018*), and the mechanical strain quantification is constricted to the superficial regions of the tissues. Tracking physical markers or speckles fixed on the sample surface is widely used to assess mechanical strain distribution on the tissue surface. Because of small size of the markers or speckles, less effect will be caused during the mechanical strain measurement. However, physical markers or speckles may move separately from the tissues and result in underestimated mechanical strain of the tissues (*O'Connell et al., 2007*). Nowadays, an increasing number of new techniques are arising. An intensity matching image registration method together with loaded and unloaded sequential micro-CT configurations have been developed and validated to measure mechanical strain fields in whole rat vertebrae (*Hardisty & Whyne, 2009*). With the technique development of mechanical strain measurement in biology, DVC has been extended to almost any imaging technology. DIC was applied to analyze the mechanical strain of rat Achilles tendons *ex vivo* using US images (*Okotie et al., 2012*). New methods with high resolution and speed should be developed with combined techniques including DVC and fast sequential micro-CT imaging for mechanical strain measurement in biological tissues. Color images are also proposed in DVC to improve the accuracy in the measurement of small mechanical strains, just as judging small strains in DIC (*Hassan et al., 2016*).

Recently, multi-scale mechanical strain measurement techniques have been utilized to provide a comprehensive overview of the mechanical strain evolution and distribution ranging from molecule-scale to tissue-scale mechanical strains. For example, synchrotron X-ray facilities have been used for tissue structure study in multiple length scales. When coupled with *in situ* loading, the techniques can be used to evaluate mechanical strains down to nanoscale. Imaging of these structures under tension (*Bianchi et al., 2016*; *Gustafsson et al., 2018*; *Zimmermann et al., 2014*), compression (*Bergstrom et al., 2017*; *Dong, Almer & Wang, 2011*) and bending (*Karunaratne et al., 2012*) can be determined for strain assessment. Gustafsson et al. combined global mechanical strain measurement with micro-scale tissue strain measurement and nano-scale collagen and mineral strain measurement in bovine cortical bone (*Gustafsson et al., 2018*). Similarly, an improved DIC was developed for the large strain measurement of cell substrate accurately (*He et al., 2018*), and the deformation of cells and their collagen constructs were assessed with scanning

electron microscopy in a different study (*Leung et al., 2018*). In addition, the strains in deformed porcine meniscus from macroscale tissue to microscale cell were evaluated using DVC analysis of confocal microscopy images (*Upton et al., 2008*). Also, based on varying interactions between proteins in tissues and introduced peptides during the deformation of tissues, biochemical approaches with peptides were also conducted for the assessment of tissues' mechanical strain (*Arnoldini, 2017*; *Kubow et al., 2015*).

Developing a real-time mechanical strain testing system that offers transient and high-quality images of mechanical strain fields is essential for clinical use. Combining different methods of mechanical strain measurement provides potential prospects. DVC, an image processing method, was applied to MR images for the quantification of intra-tissue strain fields of intra-tissue (*Bey et al., 2002b*). Confocal microscopy was used to track and capture images of fluorescently labeled cells in rat growth plates *in vitro* with applied mechanical strains and the local mechanical strain patterns were quantified using the DVC image processing approach (*Villemure et al., 2007*). In addition, a new system with the DVC image processing was developed and validated for direct internal mechanical strain measurement in connective tissues under controlled loads (*Doehring, Kahelin & Vesely, 2009*).

To reduce radiation dose and X-ray damage, extra effort should be given to design experiments for CT-based mechanical strain measurement both *in vivo* and *ex vivo*. Compared with MRI, X-ray CT mechanical strain examination is typically faster and is less prone to noise. With the evolution of testing techniques of mechanical strain, an algorithm, a mechanical strain estimation technique is presented to enhance the accuracy of mechanical strain evaluation, by directly estimating mechanical strain fields without previously first estimating displacements (*Boyle et al., 2014*). Another study showed that 2D image processing DIC offers the same mechanical strain accuracy as golden standard strain gauges under ideal conditions (*Lee, Take & Hoult, 2012*), and pointwise correlation algorithm DIC showed better mechanical strain preciseness than the traditional subset-based correlation algorithm DIC (*Jin, 2005*). First-order algorithm could significantly reduce strain measurement error, with MR images of canine knee menisci and porcine intervertebral discs (*Gilchrist et al., 2004*). Moreover, an iterative non-linear curve-fitting algorithm was introduced to test rat myocardium mechanical strain with 3D high-frequency US speckle tracking (*Yap et al., 2015*).

In conclusion, besides electro-based mechanical strain measurement techniques, almost all the other techniques for the evaluation of mechanical strains in tissues are based on the imaging of the tissues and analysis algorithms for the mechanical strain calculation from the images. Thus, combining and developing DVC with imaging techniques including high-speed and universal X-ray micro-CT modalities is a promising way for 3D mechanical strain evaluation of tissues.

ADDITIONAL INFORMATION AND DECLARATIONS

Author Contributions

- Lingwei Huang prepared figures and/or tables, authored or reviewed drafts of the paper, approved the final draft.
- Rami K. Korhonen, Mikael J. Turunen and Mikko A.J. Finnilä authored or reviewed drafts of the paper, approved the final draft.

Data Availability

The following information was supplied regarding data availability:

This article is a literature review and therefore did not generate, collect or analyze any raw data or code.

REFERENCES

Al Nazer R, Klodowski A, Rantalainen T, Heinonen A, Sievänen H, Mikkola A. 2008. Analysis of dynamic strains in tibia during human locomotion based on flexible multibody approach integrated with magnetic resonance imaging technique. *Multibody System Dynamics* **20(4)**:287–306 DOI 10.1007/s11044-008-9120-8.

Al Nazer R, Lanovaz J, Kawalilak C, Johnston JD, Kontulainen S. 2012. Direct in vivo strain measurements in human bone-a systematic literature review. *Journal of Biomechanics* **45(1)**:27–40 DOI 10.1016/j.jbiomech.2011.08.004.

Amundsen BH, Helle-Valle T, Edvardsen T, Torp H, Crosby J, Lyseggen E, Stoylen A, Ihlen H, Lima JA, Smiseth OA, Slørdahl SA. 2006. Noninvasive myocardial strain measurement by speckle tracking echocardiography: validation against sonomicrometry and tagged magnetic resonance imaging. *Journal of the American College of Cardiology* **47(4)**:789–793 DOI 10.1016/j.jacc.2005.10.040.

Andre F, Robbers-Visser D, Helling-Bakki A, Foll A, Voss A, Katus HA, Helbing WA, Buss SJ, Eichhorn JG. 2016. Quantification of myocardial deformation in children by cardiovascular magnetic resonance feature tracking: determination of reference values for left ventricular strain and strain rate. *Journal of Cardiovascular Magnetic Resonance* **19**:Article 8 DOI 10.1186/s12968-016-0310-x.

Arnoldini S. 2017. Use of fibronectin binding peptides to measure mechanical strain of fibronectin fibers in tissue. Doctoral Thesis, ETH Zurich.

Axel L. 1997. Noninvasive measurement of cardiac strain with MRI. *Advances in Experimental Medicine and Biology* **430**:249–256 DOI 10.1007/978-1-4615-5959-7_21.

Bartell LR, Fortier LA, Bonassar LJ, Cohen I. 2015. Measuring microscale strain fields in articular cartilage during rapid impact reveals thresholds for chondrocyte death and a protective role for the superficial layer. *Journal of Biomechanics* **48(12)**:3440–3446 DOI 10.1016/j.jbiomech.2015.05.035.

Bay BK. 1995. Texture correlation: a method for the measurement of detailed strain distributions within trabecular bone. *Journal of Orthopaedic Research* **13(2)**:258–267 DOI 10.1002/jor.1100130214.

Bay BK. 2008. Methods and applications of digital volume correlation. *The Journal of Strain Analysis for Engineering Design* **43(8)**:745–760 DOI 10.1243/03093247jsa436.

Bay BK, Yerby SA, McLain RF, Toh E. 1999. Measurement of strain distributions within vertebral body sections by texture correlation. *Spine* **24(1)**:10–17 DOI 10.1097/00007632-199901010-00004.

Begonia MT, Dallas M, Vizcarra B, Liu Y, Johnson ML, Thiagarajan G. 2015. Non-contact strain measurement in the mouse forearm loading model using digital image correlation (DIC). *Bone* **81**:593–601 DOI 10.1016/j.bone.2015.09.007.

Bergstrom I, Kerns JG, Tornqvist AE, Perdikouri C, Mathavan N, Koskela A, Henriksson HB, Tuukkanen J, Andersson G, Isaksson H, Goodship AE, Windahl SH. 2017. Compressive loading of the murine tibia reveals site-specific micro-scale differences in adaptation and maturation rates of bone. *Osteoporosis International* **28(3)**:1121–1131 DOI 10.1007/s00198-016-3846-6.

Bey MJ, Song HK, Wehrli FW, Soslowsky LJ. 2002a. Intratendinous strain fields of the intact supraspinatus tendon: the effect of glenohumeral joint position and tendon region. *Journal of Orthopaedic Research* **20(4)**:869–874 DOI 10.1016/S0736-0266(01)00177-2.

Bey MJ, Song HK, Wehrli SW, Soslowsky LJ. 2002b. A noncontact, nondestructive method for quantifying intratissue deformations and strains. *Journal of Biomechanical Engineering* **124(2)**:253–258 DOI 10.1115/1.1449917.

Bhatnagar T, Liu J, Yung A, Cripton PA, Kozlowski P, Oxland T. 2016. In vivo measurement of cervical spinal cord deformation during traumatic spinal cord injury in a rodent model. *Annals of Biomedical Engineering* **44(4)**:1285–1298 DOI 10.1007/s10439-015-1412-6.

Bianchi F, Hofmann F, Smith AJ, Thompson MS. 2016. Probing multi-scale mechanical damage in connective tissues using X-ray diffraction. *Acta Biomaterialia* **45**:321–327 DOI 10.1016/j.actbio.2016.08.027.

Bihari P, Shelke A, Nwe TH, Mularczyk M, Nelson K, Schmandra T, Knez P, Schmitz-Rixen T. 2013. Strain measurement of abdominal aortic aneurysm with real-time 3D ultrasound speckle tracking. *European Journal of Vascular and Endovascular Surgery* **45(4)**:315–323 DOI 10.1016/j.ejvs.2013.01.004.

Boekhoven RW, Rutten MC, Van Sambeek MR, Van de Vosse FN, Lopata RG. 2014. Echo-computed tomography strain imaging of healthy and diseased carotid specimens. *Ultrasound in Medicine and Biology* **40(6)**:1329–1342 DOI 10.1016/j.ultrasmedbio.2013.11.026.

Boyle JJ, Kume M, Wyczalkowski MA, Taber LA, Pless RB, Xia Y, Genin GM, Thomopoulos S. 2014. Simple and accurate methods for quantifying deformation, disruption, and development in biological tissues. *Journal of the Royal Society Interface* **11**(**100**):Article 20140685 DOI 10.1098/rsif.2014.0685.

Bravo T, Tersalvi A, Tosi A. 1992. Comparison of SiOx and polyimide as a dielectric layer on stainless steel in thin-film pressure sensor manufacture. *Sensors and Actuators A: Physical* **32**(**1–3**):611–615 DOI 10.1016/0924-4247(92)80052-5.

Brown AN, McKinley TO, Bay BK. 2002. Trabecular bone strain changes associated with subchondral bone defects of the tibial plateau. *Journal of Orthopaedic Trauma* **16**(**9**):638–643 DOI 10.1097/00005131-200210000-00005.

Bruno L, Bianco G, Fazio MA. 2018. A multi-camera speckle interferometer for dynamic full-field 3D displacement measurement: validation and inflation testing of a human eye sclera. *Optics and Lasers in Engineering* **107**:91–101 DOI 10.1016/j.optlaseng.2018.03.012.

Burny F, Donkerwolcke M, Bourgois R, Domb M, Saric O. 1984. Twenty years experience in fracture healing measurement with strain gauges. *Orthopedics* **7**(**12**):1823–1826.

Butler DL, Sheh MY, Stouffer DC, Samaranayake VA, Levy MS. 1990. Surface strain variation in human patellar tendon and knee cruciate ligaments. *Journal of Biomechanical Engineering* **112**(**1**):38–45 DOI 10.1115/1.2891124.

Cehreli MC, Akkocaoglu M, Comert A, Tekdemir I, Akca K. 2005. Human ex vivo bone tissue strains around natural teeth vs. immediate oral implants. *Clinical Oral Implants Research* **16**(**5**):540–548 DOI 10.1111/j.1600-0501.2005.01140.x.

Chan DD, Knutsen AK, Lu YC, Yang SH, Magrath E, Wang WT, Bayly PV, Butman JA, Pham DL. 2018. Statistical characterization of human brain deformation during mild angular acceleration measured in vivo by tagged magnetic resonance imaging. *Journal of Biomechanical Engineering* **140**(**10**):Article 101005 DOI 10.1115/1.4040230.

Chernak Slane L, Thelen DG. 2014. The use of 2D ultrasound elastography for measuring tendon motion and strain. *Journal of Biomechanics* **47**(**3**):750–754 DOI 10.1016/j.jbiomech.2013.11.023.

Choudhari C, Herblum R, Akens MK, Moore S, Hardisty M, Whyne CM. 2016. Post-euthanasia micro-computed tomography-based strain analysis is able to represent quasi-static in vivo behavior of whole vertebrae. *Proceedings of the Institution of Mechanical Engineers Part H: Journal of Engineering in Medicine* **230**(**9**):900–904 DOI 10.1177/0954411916658679.

Coudrillier B, Geraldes DM, Vo NT, Atwood R, Reinhard C, Campbell IC, Raji Y, Albon J, Abel RL, Ethier CR. 2016. Phase-contrast micro-computed tomography measurements of the intraocular pressure-induced deformation of the porcine lamina cribrosa. *IEEE Transactions on Medical Imaging* **35**(**4**):988–999 DOI 10.1109/TMI.2015.2504440.

Cyganik L, Binkowski M, Kokot G, Rusin T, Popik P, Bolechala F, Nowak R, Wrobel Z, John A. 2014. Prediction of Youngs modulus of trabeculae in microscale

using macro-scales relationships between bone density and mechanical properties. *Journal of the Mechanical Behavior of Biomedical Materials* **36**:120–134 DOI 10.1016/j.jmbbm.2014.04.011.

Dai XJ, Yang FJ, Chen ZN, Shao XX, He XY. 2015. Strain field estimation based on digital image correlation and radial basis function. *Optics and Lasers in Engineering* **65**:64–72 DOI 10.1016/j.optlaseng.2014.05.007.

Danesi V, Tozzi G, Cristofolini L. 2016. Application of digital volume correlation to study the efficacy of prophylactic vertebral augmentation. *Clinical Biomechanics* **39**:14–24 DOI 10.1016/j.clinbiomech.2016.07.010.

Davies HMS, Mccarthy RN, Jeffcott LB. 1993. Surface strain on the dorsal metacarpus of thoroughbreds at different speeds and gaits. *Acta Anatomica* **146(2–3)**:148–153.

Derpa VF, Koch R, Mollers M, Hammer K, Oelmeierde Murcia K, Koster HA, Falkenberg MK, Braun J, Klockenbusch W, Schmitz R. 2018. Comparison of longitudinal and apical foetal speckle tracking echocardiography using tissue motion annular displacement and segmental longitudinal strain. *Ultrasound in Medicine & Biology* **45(1)**:233–245 DOI 10.1016/j.ultrasmedbio.2018.09.013.

DiGiampaolo E, DiCarlofelice A, Gregori A. 2017. An RFID—enabled wireless strain gauge sensor for static and dynamic structural monitoring. *IEEE Sensors Journal* **17(2)**:286–294 DOI 10.1109/Jsen.2016.2631259.

Doehring TC, Kahelin M, Vesely I. 2009. Direct measurement of nonuniform large deformations in soft tissues during uniaxial extension. *Journal of Biomechanical Engineering* **131(6)**:Article 061001 DOI 10.1115/1.3116155.

Dong XN, Almer JD, Wang X. 2011. Post-yield nanomechanics of human cortical bone in compression using synchrotron X-ray scattering techniques. *Journal of Biomechanics* **44(4)**:676–682 DOI 10.1016/j.jbiomech.2010.11.003.

Ekenman I, Halvorsen K, Westblad P, Fellander-Tsai L, Rolf C. 1998. The reliability and validity of an instrumented staple system for in vivo measurement of local bone deformation. An in vitro study. *Scandinavian Journal of Medicine & Science in Sports* **8(3)**:172–176.

Enns-Bray WS, Ariza O, Gilchrist S, Widmer Soyka RP, Vogt PJ, Palsson H, Boyd SK, Guy P, Cripton PA, Ferguson SJ, Helgason B. 2016. Morphology based anisotropic finite element models of the proximal femur validated with experimental data. *Medical Engineering & Physics* **38(11)**:1339–1347 DOI 10.1016/j.medengphy.2016.08.010.

Feola AJ, Coudrillier B, Mulvihill J, Geraldes DM, Vo NT, Albon J, Abel RL, Samuels BC, Ethier CR. 2017. Deformation of the lamina cribrosa and optic nerve due to changes in cerebrospinal fluid pressure. *Investigative Ophthalmology & Visual Science* **58(4)**:2070–2078 DOI 10.1167/iovs.16-21393.

Fick JM, Ronkainen AP, Herzog W, Korhonen RK. 2015. Site-dependent biomechanical responses of chondrocytes in the rabbit knee joint. *Journal of Biomechanics* **48(15)**:4010–4019 DOI 10.1016/j.jbiomech.2015.09.049.

Fick JM, Ronkainen AP, Madden R, Sawatsky A, Tiitu V, Herzog W, Korhonen RK. 2016. Early in situ changes in chondrocyte biomechanical responses due to a partial

meniscectomy in the lateral compartment of the mature rabbit knee joint. *Journal of Biomechanics* **49**(**16**):4057–4064 DOI 10.1016/j.jbiomech.2016.10.039.

Fleming BC, Beynnon BD. 2004. In vivo measurement of ligament/tendon strains and forces: a review. *Annals of Biomedical Engineering* **32**(**3**):318–328.

Frost HM. 2004. A 2003 update of bone physiology and Wolff's Law for clinicians. *Angle Orthodontist* **74**(**1**):3–15.

Fung A, Loundagin LL, Edwards WB. 2017. Experimental validation of finite element predicted bone strain in the human metatarsal. *Journal of Biomechanics* **60**:22–29 DOI 10.1016/j.jbiomech.2017.06.010.

Gautier E, Perren SM, Cordey J. 2000. Strain distribution in plated and unplated sheep tibia an in vivo experiment. *Injury* **31**(**Suppl 3**):C37–C44 DOI 10.1016/S0020-1383(00)80030-3.

Germanakis I, Gardiner H. 2012. Assessment of fetal myocardial deformation using speckle tracking techniques. *Fetal Diagnosis and Therapy* **32**(**1–2**):39–46 DOI 10.1159/000330378.

Germaneau A, Doumalin P, Dupré J-C. 2008. Comparison between X-ray micro-computed tomography and optical scanning tomography for full 3D strain measurement by digital volume correlation. *NDT & E International* **41**(**6**):407–415 DOI 10.1016/j.ndteint.2008.04.001.

Gilchrist CL, Xia JQ, Setton LA, Hsu EW. 2004. High-resolution determination of soft tissue deformations using MRI and first-order texture correlation. *IEEE Transactions on Medical Imaging* **23**(**5**):546–553 DOI 10.1109/tmi.2004.825616.

Gilja OH, Heimdal A, Hausken T, Gregersen H, Matre K, Berstad A, Odegaard S. 2002. Strain during gastric contractions can be measured using Doppler ultrasonography. *Ultrasound in Medicine and Biology* **28**(**11–12**):1457–1465 DOI 10.1016/S0301-5629(02)00614-2.

Gillard F, Boardman R, Mavrogordato M, Hollis D, Sinclair I, Pierron F, Browne M. 2014. The application of digital volume correlation (DVC) to study the microstructural behaviour of trabecular bone during compression. *Journal of The Mechanical Behavior of Biomedical Materials* **29**(**SI**):480–499 DOI 10.1016/j.jmbbm.2013.09.014.

Grassi L, Isaksson H. 2015. Extracting accurate strain measurements in bone mechanics: a critical review of current methods. *Journal of The Mechanical Behavior of Biomedical Materials* **50**:43–54 DOI 10.1016/j.jmbbm.2015.06.006.

Gustafsson A, Mathavan N, Turunen MJ, Engqvist J, Khayyeri H, Hall SA, Isaksson H. 2018. Linking multiscale deformation to microstructure in cortical bone using in situ loading, digital image correlation and synchrotron X-ray scattering. *Acta Biomaterialia* **69**:323–331 DOI 10.1016/j.actbio.2018.01.037.

Hacker SP, Schall F, Niemeyer F, Wolf N, Ignatius A, Durselen L. 2018. Do prophylactic knee braces protect the knee against impacts or tibial moments? An in vitro multisensory study. *The Orthopaedic Journal of Sports Medicine* **6**(**11**):Article 2325967118805399 DOI 10.1177/2325967118805399.

Halonen KS, Mononen ME, Jurvelin JS, Toyras J, Salo J, Korhonen RK. 2014. Deformation of articular cartilage during static loading of a knee joint— experimental and finite element analysis. *Journal of Biomechanics* **47(10)**:2467–2474 DOI 10.1016/j.jbiomech.2014.04.013.

Hardisty MR, Whyne CM. 2009. Whole bone strain quantification by image registration: a validation study. *Journal of Biomechanical Engineering* **131(6)**:Article 064502 DOI 10.1115/1.3127249.

Hassan GM, Dyskin AV, MacNish CK, Dinh NV. 2016. A comparative study of techniques of distant reconstruction of displacement and strain fields using the DISTRESS simulator. *Optik* **127(23)**:11288–11305 DOI 10.1016/j.ijleo.2016.09.026.

He H, Zhou R, Zou Y, Huang X, Li J. 2018. A comprehensive method for accurate strain distribution measurement of cell substrate subjected to large deformation. *Journal of Healthcare Engineering* **2018**:Article 8504273 DOI 10.1155/2018/8504273.

Heijne A, Fleming BC, Renstrom PA, Peura GD, Beynnon BD, Werner S. 2004. Strain on the anterior cruciate ligament during closed kinetic chain exercises. *Medicine and Science in Sports and Exercise* **36(6)**:935–941 DOI 10.1249/01.mss.0000128185.55587.a3.

Herbots L, Maes F, D'Hooge J, Claus P, Dymarkowski S, Mertens P, Mortelmans L, Bijnens B, Bogaert J, Rademakers FE, Sutherland GR. 2004. Quantifying myocardial deformation throughout the cardiac cycle: a comparison of ultrasound strain rate, grey-scale M-mode and magnetic resonance imaging. *Ultrasound in Medicine and Biology* **30(5)**:591–598 DOI 10.1016/j.ultrasmedbio.2004.02.003.

Hirsch S, Klatt D, Freimann F, Scheel M, Braun J, Sack I. 2013. In vivo measurement of volumetric strain in the human brain induced by arterial pulsation and harmonic waves. *Magnetic Resonance in Medicine* **70(3)**:671–683 DOI 10.1002/mrm.24499.

Hoc T, Henry L, Verdier M, Aubry D, Sedel L, Meunier A. 2006. Effect of microstructure on the mechanical properties of Haversian cortical bone. *Bone* **38(4)**:466–474 DOI 10.1016/j.bone.2005.09.017.

Huang LW, Ren L, Yang PF, Shang P. 2015. Response of osteoblasts to the stimulus of fluid flow. *Critical Reviews in Eukaryotic Gene Expression* **25(2)**:153–162 DOI 10.1615/CritRevEukaryotGeneExpr.2015013564.

Hussein AI, Barbone PE, Morgan EF. 2012. Digital volume correlation for study of the mechanics of whole bones. *Procedia IUTAM* **4**:116–125 DOI 10.1016/j.piutam.2012.05.013.

Jacobs CR, Temiyasathit S, Castillo AB. 2010. Osteocyte mechanobiology and pericellular mechanics. *Annual Review of Biomedical Engineering* **12**:369–400 DOI 10.1146/annurev-bioeng-070909-105302.

Jin H. 2005. Theoretical development for pointwise digital image correlation. *Optical Engineering* **44(6)**:Article 067003 DOI 10.1117/1.1928908.

Kahnjetter ZL, Chu TC. 1990. 3-Dimensional displacement measurements using digital image correlation and photogrammic analysis. *Experimental Mechanics* **30(1)**:10–16 DOI 10.1007/Bf02322695.

Karunaratne A, Esapa CR, Hiller J, Boyde A, Head R, Bassett JH, Terrill NJ, Williams GR, Brown MA, Croucher PI, Brown SD, Cox RD, Barber AH, Thakker RV, Gupta HS. 2012. Significant deterioration in nanomechanical quality occurs through incomplete extrafibrillar mineralization in rachitic bone: evidence from in-situ synchrotron X-ray scattering and backscattered electron imaging. *Journal of Bone and Mineral Research* **27**(**4**):876–890 DOI 10.1002/jbmr.1495.

Kim DG, Brunski JB, Nicolella DP. 2005. Microstrain fields for cortical bone in uniaxial tension: optical analysis method. *Proceedings of the Institution of Mechanical Engineers Part H: Journal of Engineering in Medicine* **219**(**2**):119–128 DOI 10.1243/095441105X9291.

Kolaczek S, Hewison C, Caterine S, Ragbar MX, Getgood A, Gordon KD. 2016. Analysis of 3D strain in the human medial meniscus. *Journal of the Mechanical Behavior of Biomedical Materials* **63**:470–475 DOI 10.1016/j.jmbbm.2016.06.001.

Kubow KE, Vukmirovic R, Zhe L, Klotzsch E, Smith ML, Gourdon D, Luna S, Vogel V. 2015. Mechanical forces regulate the interactions of fibronectin and collagen I in extracellular matrix. *Nature Communications* **6**:Article 8026 DOI 10.1038/ncomms9026.

Kuo PL, Li PC, Shun CT, Lai JS. 1999. Strain measurements of rabbit Achilles tendons by ultrasound. *Ultrasound in Medicine and Biology* **25**(**8**):1241–1250 DOI 10.1016/S0301-5629(99)00078-2.

Lee WN, Qian Z, Tosti CL, Brown TR, Metaxas DN, Konofagou EE. 2008. Preliminary validation of angle-independent myocardial elastography using MR tagging in a clinical setting. *Ultrasound in Medicine and Biology* **34**(**12**):1980–1997 DOI 10.1016/j.ultrasmedbio.2008.05.007.

Lee C, Take WA, Hoult NA. 2012. Optimum accuracy of two-dimensional strain measurements using digital image correlation. *Journal of Computing in Civil Engineering* **26**(**6**):795–803 DOI 10.1061/(asce)cp.1943-5487.0000182.

Les CM, Stover SM, Taylor KT, Keyak JH, Willits NH. 1998. Ex vivo simulation of in vivo strain distributions in the equine metacarpus. *Equine Veterinary Journal* **30**(**3**):260–266 DOI 10.1111/j.2042-3306.1998.tb04498.x.

Leung S, McGlashan SR, Musson DSP, Cornish J, Anderson IA, Shim VBK. 2018. Investigations of strain fields in 3D hydrogels under dynamic confined loading. *Journal of Medical and Biological Engineering* **38**(**3**):514–522 DOI 10.1007/s40846-017-0319-0.

Liang Y, Zhu H, Friedman MH. 2008. Estimation of the transverse strain tensor in the arterial wall using IVUS image registration. *Ultrasound in Medicine and Biology* **34**(**11**):1832–1845 DOI 10.1016/j.ultrasmedbio.2008.04.005.

Lima JA, Jeremy R, Guier W, Bouton S, Zerhouni EA, McVeigh E, Buchalter MB, Weisfeldt ML, Shapiro EP, Weiss JL. 1993. Accurate systolic wall thickening by nuclear magnetic resonance imaging with tissue tagging: correlation with sonomicrometers in normal and ischemic myocardium. *Journal of the American College of Cardiology* **21**(**7**):1741–1751 DOI 10.1016/0735-1097(93)90397-j.

Ling HY, Zheng YP, Patil SG. 2007. Strain dependence of ultrasound speed in bovine articular cartilage under compression in vitro. *Ultrasound in Medicine and Biology* **33(10)**:1599–1608 DOI 10.1016/j.ultrasmedbio.2007.04.015.

Lisong Z, Soyoun J, Brandon E, Jackson TN. 2006. Flexible substrate micro-crystalline silicon and gated amorphous silicon strain sensors. *IEEE Transactions on Electron Devices* **53(2)**:380–385 DOI 10.1109/ted.2005.861727.

Mannelli L, Wilson GJ, Dubinsky TJ, Potter CA, Bhargava P, Cuevas C, Linnau KF, Kolokythas O, Gunn ML, Maki JH. 2012. Assessment of the liver strain among cirrhotic and normal livers using tagged MRI. *Journal of Magnetic Resonance Imaging* **36(6)**:1490–1495 DOI 10.1002/jmri.23743.

Mansfield JC, Bell JS, Winlove CP. 2015. The micromechanics of the superficial zone of articular cartilage. *Osteoarthritis Cartilage* **23(10)**:1806–1816 DOI 10.1016/j.joca.2015.05.030.

Markolf KL, Willems MJ, Jackson SR, Finerman GA. 1998. In situ calibration of miniature sensors implanted into the anterior cruciate ligament part I: strain measurements. *Journal of Orthopaedic Research* **16(4)**:455–463 DOI 10.1002/jor.1100160410.

Marks L, Teng S, Artun J, Herring S. 1997. Reaction strains on the condylar neck during mastication and maximum muscle stimulation in different condylar positions: an experimental study in the miniature pig. *Journal of Dental Research* **76(7)**:1412–1420 DOI 10.1177/00220345970760071201.

McKinley TO, Bay BK. 2001. Trabecular bone strain changes associated with cartilage defects in the proximal and distal tibia. *Journal of Orthopaedic Research* **19(5)**:906–913 DOI 10.1016/S0736-0266(01)00011-0.

McKinley TO, Bay BK. 2003. Trabecular bone strain changes associated with subchondral stiffening of the proximal tibia. *Journal of Biomechanics* **36(2)**:155–163 DOI 10.1016/s0021-9290(02)00386-x.

McKinley TO, English DK, Bay BK. 2003. Trabecular bone strain changes resulting from partial and complete meniscectomy. *Clinical Orthopaedics and Related Research* **(407)**:259–267 DOI 10.1097/00003086-200302000-00035.

McVeigh ER, Zerhouni EA. 1991. Noninvasive measurement of transmural gradients in myocardial strain with MR imaging. *Radiology* **180(3)**:677–683 DOI 10.1148/radiology.180.3.1871278.

Milgrom C, Finestone A, Levi Y, Simkin A, Ekenman I, Mendelson S, Millgram M, Nyska M, Benjuya N, Burr D. 2000a. Do high impact exercises produce higher tibial strains than running? *British Journal of Sports Medicine* **34(3)**:195–199 DOI 10.1136/bjsm.34.3.195.

Milgrom C, Finestone A, Simkin A, Ekenman I, Mendelson S, Millgram M, Nyska M, Larsson E, Burr D. 2000b. In-vivo strain measurements to evaluate the strengthening potential of exercises on the tibial bone. *Journal of Bone and Joint Durgery-British Volume* **82(4)**:591–594 DOI 10.1302/0301-620X.82B4.9677.

Moo EK, Sibole SC, Han SK, Herzog W. 2018. Three-dimensional micro-scale strain mapping in living biological soft tissues. *Acta Biomaterialia* **70**:260–269 DOI 10.1016/j.actbio.2018.01.048.

Muraru D, Niero A, Rodriguez-Zanella H, Cherata D, Badano L. 2018. Three-dimensional speckle-tracking echocardiography: benefits and limitations of integrating myocardial mechanics with three-dimensional imaging. *Cardiovascular Diagnosis and Therapy* **8(1)**:101–117 DOI 10.21037/cdt.2017.06.01.

Negishi K, Lucas S, Negishi T, Hamilton J, Marwick TH. 2013. What is the primary source of discordance in strain measurement between vendors: imaging or analysis? *Ultrasound in Medicine Biology* **39(4)**:714–720 DOI 10.1016/j.ultrasmedbio.2012.11.021.

Novitskaya E, Zin C, Chang N, Cory E, Chen P, D'Lima D, Sah RL, McKittrick J. 2014. Creep of trabecular bone from the human proximal tibia. *Materials Science and Engineering: C* **40**:219–227 DOI 10.1016/j.msec.2014.03.057.

O'Connell GD, Johannessen W, Vresilovic EJ, Elliott DM. 2007. Human internal disc strains in axial compression measured noninvasively using magnetic resonance imaging. *Spine* **32(25)**:2860–2868 DOI 10.1097/BRS.0b013e31815b75fb.

Okotie G, Duenwald-Kuehl S, Kobayashi H, Wu MJ, Vanderby R. 2012. Tendon strain measurements with dynamic ultrasound images: evaluation of digital image correlation. *Journal of Biomechanical Engineering* **134(2)**:Article 024504 DOI 10.1115/1.4006116.

O'Neill PJ, Parks BG, Walsh R, Simmons LM, Miller SD. 2007. Excursion and strain of the superficial peroneal nerve during inversion ankle sprain. *Journal of Bone and Joint Surgery-American Volume* **89(5)**:979–986 DOI 10.2106/JBJS.F.00440.

Ozeki S, Yasuda K, Kaneda K, Yamakoshi K, Yamanoi T. 2002. Simultaneous strain measurement with determination of a zero strain reference for the medial and lateral ligaments of the ankle. *Foot & Ankle International* **23(9)**:825–832 DOI 10.1177/107110070202300909.

Pan B, Qian KM, Xie HM, Asundi A. 2009. Two-dimensional digital image correlation for in-plane displacement and strain measurement: a review. *Measurement Science and Technology* **20(6)**:Article 062001 DOI 10.1088/0957-0233/20/6/062001.

Papademetris X, Sinusas AJ, Dione DP, Duncan JS. 2001. Estimation of 3D left ventricular deformation from echocardiography. *Medical Image Analysis* **5(1)**:17–28 DOI 10.1016/S1361-8415(00)00022-0.

Peltonen J, Cronin NJ, Stenroth L, Finni T, Avela J. 2013. Viscoelastic properties of the Achilles tendon in vivo. *Springerplus* **2**:Article 212 DOI 10.1186/2193-1801-2-212.

Perk G, Tunick PA, Kronzon I. 2007. Non-Doppler two-dimensional strain imaging by echocardiography—from technical considerations to clinical applications. *Journal of the American Society of Echocardiography* **20(3)**:234–243 DOI 10.1016/j.echo.2006.08.023.

Pierce EL, Bloodworth CHT, Naran A, Easley TF, Jensen MO, Yoganathan AP. 2016. Novel method to track soft tissue deformation by micro-computed tomography: application to the mitral valve. *Annals of Biomedical Engineering* **44(7)**:2273–2281 DOI 10.1007/s10439-015-1499-9.

Pintar FA, Yoganandan N, Pesigan M, Reinartz J, Sances Jr A, Cusick JF. 1995.
Cervical vertebral strain measurements under axial and eccentric loading. *Journal of Biomechanical Engineering* **117**(**4**):474–478 DOI 10.1115/1.2794210.

Pozzi A, Tonks CA, Ling HY. 2010. Femorotibial contact mechanics and meniscal strain after serial meniscectomy. *Veterinary Surgery* **39**(**4**):482–488 DOI 10.1111/j.1532-950X.2010.00668.x.

Rabkin BA, Szivek JA, Schonfeld JE, Halloran BP. 2001. Long-term measurement of bone strain in vivo: the rat tibia. *Journal of Biomedical Materials Research* **58**(**3**):277–281 DOI 10.1002/1097-4636(2001)58:3<277::AID-JBM1017>3.0.CO;2-T.

Rodriguez D, Moreno V, Gallas M, Abeleira MT, Suarez D. 2004. In-plane electronic speckle pattern of interference (ESPI) with optical fibre system applied to the study of the human jaw. *Medical Engineering & Physics* **26**(**5**):371–378 DOI 10.1016/j.medengphy.2004.02.010.

Rolf C, Westblad P, Ekenman I, Lundberg A, Murphy N, Lamontagne M, Halvorsen K. 1997. An experimental in vivo method for analysis of local deformation on tibia, with simultaneous measures of ground reaction forces, lower extremity muscle activity and joint motion. *Scandinavian Journal of Medicine & Science in Sports* **7**(**3**):144–151 DOI 10.1111/j.1600-0838.1997.tb00131.x.

Sekitani T, Zschieschang U, Klauk H, Someya T. 2010. Flexible organic transistors and circuits with extreme bending stability. *Nature Materials* **9**(**12**):1015–1022 DOI 10.1038/nmat2896.

Sheehan FT, Drace JE. 2000. Human patellar tendon strain. A noninvasive, in vivo study. *Clinical Orthopaedics and Related Research* (**370**):201–207.

Shelton JC, Katz DM. 1991. Laser interferometric techniques in orthopaedics. *Journal of Medical Engineering & Technology* **15**(**6**):209–221 DOI 10.3109/03091909109005419.

Simonetti OP, Raman SV. 2010. Straining to justify strain measurement. *JACC Cardiovasc Ular Imaging* **3**(**2**):152–154 DOI 10.1016/j.jcmg.2009.11.005.

Smith MV, Castile RM, Brophy RH, Dewan A, Bernholt D, Lake SP. 2019. Mechanical properties and microstructural collagen alignment of the ulnar collateral ligament during dynamic loading. *American Journal of Sports Medicine* **47**(**1**):151–157 DOI 10.1177/0363546518812416.

Song S, Race NS, Kim A, Zhang T, Shi R, Ziaie B. 2015. A wireless intracranial brain deformation sensing system for blast-induced traumatic brain injury. *Scientific Reports* **5**:16959 DOI 10.1038/srep16959.

Spiegel DA, Cunningham BW, Oda I, Dormans JP, McAfee PC, Drummond DS. 2000. Anterior vertebral screw strain with and without solid interspace support. *Spine* **25**(**21**):2755–2761 DOI 10.1097/00007632-200011010-00007.

Squire JC, Rogers C, Edelman ER. 1999. Measuring arterial strain induced by endovascular stents. *Medical & Biological Engineering & Computing* **37**(**6**):692–698 DOI 10.1007/BF02513369.

Steen H, Tseng KF, Goldstein SA, Carpenter JE. 1999. Harvest of patellar tendon (bone-tendon-bone) autograft for ACL reconstruction significantly alters surface

strain in the human patella. *Journal of Biomechanical Engineering* **121(2)**:229–233 DOI 10.1115/1.2835108.

Stokes OM, Theobald PS, Pugh ND, Nokes LD. 2010. Panoramic ultrasound to measure in vivo tendo Achilles strain. *Foot & Ankle International* **31(10)**:905–909 DOI 10.3113/FAI.2010.0905.

Sumi C. 2007. Ultrasonic axial strain measurement for lateral tissue deformation. *Ultrasound in Medicine and Biology* **33(11)**:1830–1837 DOI 10.1016/j.ultrasmedbio.2007.05.005.

Sun GK, Wu YP, Li H, Zhu LQ. 2018. 3D shape sensing of flexible morphing wing using fiber Bragg grating sensing method. *Optik* **156**:83–92 DOI 10.1016/j.ijleo.2017.10.159.

Sutter EG, Widmyer MR, Utturkar GM, Spritzer CE, Garrett Jr WE, DeFrate LE. 2015. In vivo measurement of localized tibiofemoral cartilage strains in response to dynamic activity. *American Journal of Sports Medicine* **43(2)**:370–376 DOI 10.1177/0363546514559821.

Szivek JA, Anderson PL, DeYoung DW. 1997. In vivo strain measurements collected using calcium phosphate ceramic-bonded strain gauges. *Journal of Investigative Surgery* **10(5)**:263–273 DOI 10.3109/08941939709032165.

Szivek JA, Gealer RG, Magee FP, Emmanual J. 1990. Preliminary development of a hydroxyapatite-backed strain gauge. *Journal of Applied Biomaterials* **1(3)**:241–248 DOI 10.1002/jab.770010307.

Szivek JA, Roberto RF, Slack JM, Majeed BS. 2002. An implantable strain measurement system designed to detect spine fusion: preliminary results from a biomechanical in vivo study. *Spine* **27(5)**:487–497 DOI 10.1097/00007632-200203010-00009.

Takano Y, Turner CH, Owan I, Martin RB, Lau ST, Forwood MR, Burr DB. 1999. Elastic anisotropy and collagen orientation of osteonal bone are dependent on the mechanical strain distribution. *Journal of Orthopaedic Research* **17(1)**:59–66 DOI 10.1002/jor.1100170110.

Tanasic I, Milic-Lemic A, Tihacek-Sojic L, Stancic I, Mitrovic N. 2012. Analysis of the compressive strain below the removable and fixed prosthesis in the posterior mandible using a digital image correlation method. *Biomechanics and Modeling in Mechanobiology* **11(6)**:751–758 DOI 10.1007/s10237-011-0348-5.

Teo KY, Dutton JC, Han B. 2010. Spatiotemporal measurement of freezing-induced deformation of engineered tissues. *Journal of Biomechanical Engineering* **132(3)**:Article 031003 DOI 10.1115/1.4000875.

Toh E, Yerby SA, Bay BK, McLain RF, Mochida J. 2006. The influence of pedicle screw placement on thoracic trabecular strain. *Spinal Cord* **44(4)**:249–253 DOI 10.1038/sj.sc.3101830.

Turunen SM, Han SK, Herzog W, Korhonen RK. 2013. Cell deformation behavior in mechanically loaded rabbit articular cartilage 4 weeks after anterior cruciate ligament transection. *Osteoarthritis Cartilage* **21(3)**:505–513 DOI 10.1016/j.joca.2012.12.001.

Upton ML, Gilchrist CL, Guilak F, Setton LA. 2008. Transfer of macroscale tissue strain to microscale cell regions in the deformed meniscus. *Biophysical Journal* **95(4)**:2116–2124 DOI 10.1529/biophysj.107.126938.

Van Slochteren FJ, Van der Spoel TI, Hansen HH, Bovendeerd PH, Doevendans PA, Sluijter JP, Chamuleau SA, De Korte CL. 2014. Layer-specific radiofrequency ultrasound-based strain analysis in a porcine model of ischemic cardiomyopathy validated by a geometric model. *Ultrasound in Medicine and Biology* **40(2)**:378–388 DOI 10.1016/j.ultrasmedbio.2013.09.030.

Villemure I, Cloutier L, Matyas JR, Duncan NA. 2007. Non-uniform strain distribution within rat cartilaginous growth plate under uniaxial compression. *Journal of Biomechanics* **40(1)**:149–156 DOI 10.1016/j.jbiomech.2005.11.008.

Wang HX, Xie HM, Wu LF, He SY. 2014. Study on the effect of DIC deformation sensor on mechanical property of substrate. *Measurement* **49**:283–288 DOI 10.1016/j.measurement.2013.12.006.

Wilson DL, Szivek JA, Anderson PL, Miera VL, Battraw GA. 2009a. A mechanical and histomorphometric analysis of bone bonding by hydroxyapatite-coated strain gages. *Journal of Investigative Surgery* **11(1)**:29–48 DOI 10.3109/08941939809032178.

Wilson NA, Press JM, Zhang LQ. 2009b. In vivo strain of the medial vs. lateral quadriceps tendon in patellofemoral pain syndrome. *Journal of Applied Physiology* **107(2)**:422–428 DOI 10.1152/japplphysiol.00024.2009.

Wright TW, Glowczewskie F, Wheeler D, Miller G, Cowin D. 1996. Excursion and strain of the median nerve. *Journal of Bone and Joint Surgery-American* **78A(12)**:1897–1903 DOI 10.2106/00004623-199612000-00013.

Yang PF, Bruggemann GP, Rittweger J. 2011. What do we currently know from in vivo bone strain measurements in humans? *Journal of Musculoskeletal & Neuronal Interactions* **11(1)**:8–20.

Yap CH, Park DW, Dutta D, Simon M, Kim K. 2015. Methods for using 3-D ultrasound speckle tracking in biaxial mechanical testing of biological tissue samples. *Ultrasound in Medicine and Biology* **41(4)**:1029–1042 DOI 10.1016/j.ultrasmedbio.2014.10.021.

Yerby SA, Bay BK, Toh E, McLain RF, Drews MJ. 1998. The effect of boundary conditions on experimentally measured trabecular strain in the thoracic spine. *Journal of Biomechanics* **31(10)**:891–897 DOI 10.1016/S0021-9290(98)00064-5.

Younis NT, Kang B. 2011. Averaging effects of a strain gage. *Journal of Mechanical Science and Technology* **25(1)**:163–169 DOI 10.1007/s12206-010-1020-1.

Zhao P, Deng N, Li X, Ren C, Wang Z. 2014. Development of highly-sensitive and ultra-thin silicon stress sensor chips for wearable biomedical applications. *Sensors and Actuators A: Physical* **216**:158–166 DOI 10.1016/j.sna.2014.05.018.

Zhu H, Liu X, Chen L, Ma Q, Ma S. 2018. Influence of imaging configurations on the accuracy of digital image correlation measurement. *Measurement Science and Technology* **29(3)**:Article 035205 DOI 10.1088/1361-6501/aa9e6a.

Zimmermann EA, Gludovatz B, Schaible E, Busse B, Ritchie RO. 2014. Fracture resistance of human cortical bone across multiple length-scales at physiological strain rates. *Biomaterials* **35(21)**:5472–5481 DOI 10.1016/j.biomaterials.2014.03.066.